Polymer/Silica Composite Films as Luminescent Oxygen Sensors

Xin Lu, Ian Manners, and Mitchell A. Winnik*

Department of Chemistry, University of Toronto, 80 Saint George Street, Toronto, ON M5S 3H6, Canada

Received August 17, 2000; Revised Manuscript Received November 20, 2000

ABSTRACT: In this paper, we examine the influence of 10 nm diameter silica nanospheres on oxygen diffusion in films of two different amorphous polymers characterized by a low glass-transition temperature and a high oxygen permeability. The two polymers, poly(dimethylsiloxane) (PDMS) and poly(*n*-butylamino thionylphosphazene) (C_4PATP), are useful matrixes for oxygen sensors based upon luminescence quenching. In these applications, the dye platinum octaethylporphine (PtOEP), with a long-lived excited state, is incorporated into the polymer, and the presence of oxygen is registered through a quenching of the dye luminescence. For some sensor applications, these linear polymers themselves are too soft and tacky. Silica as a filler improves the mechanical properties of the matrix but perturbs the measurement of oxygen diffusion and permeation. We show that PtOEP adsorbs to the silica particles in PDMS but remains in the polymer matrix in C_4PATP. The quenching kinetics of dye fluorescence is complex in PDMS because of contributions of oxygen adsorbed to the silica surface and that dissolved in the polymer matrix. In contrast, the quenching kinetics in C_4PATP remains almost unaffected by the presence of silica. Time-scan experiments on PDMS films show good accord with Fick's laws of diffusion for films containing up to 30 wt % (16 vol %) silica. The diffusion constant, D_{O2}, is reduced but only by a factor of about two. In C_4PATP, the time-scan experiments give more complex results because the oxygen adsorbed to the surface of the silica particles serves as an additional reservoir for oxygen in the system. Because the PtOEP remains in the polymer matrix in C_4PATP, the oxygen adsorbed to the silica does not participate in quenching until it diffuses away from the particles and into the matrix.

1. Introduction

Mineral fillers are often added to polymers to improve their mechanical properties.[1] For polymers above their glass-transition temperature (T_g), the filler particles increase the modulus of the polymer; for films of these polymers, the filler improves the block resistance. When polymer films are used in sensor applications, mineral fillers are sometimes employed to improve the mechanical properties of the matrix[2−4] or as a carrier of the luminescent dye.[5,6] Here the presence of the solid particles in the composite can affect the response of the sensor in ways that are poorly understood. From an operational point of view, it may be sufficient to calibrate the sensor composite so that the response can be meaningfully interpreted. From a design point of view, it would be better to have a mechanistic understanding of how the components of the sensor interact with the filler particles and how the particles themselves affect the response of the sensor.

Optical sensors for oxygen are based upon the idea that the excited state of many dyes is rapidly quenched by proximity to an oxygen molecule. The active component of the sensor consists of a polymer with a high permeability to oxygen in which dye molecules are dissolved. When a film of this polymer is exposed to a gas or liquid containing oxygen, oxygen molecules partition between the polymer film and the external medium. One monitors the effect of oxygen in the film on the intensity or decay time of the dye luminescence. Many of the dyes employed for this purpose have lowest energy triplet states,[2−6] and the presence of oxygen is detected through measurements of phosphorescence quenching. The key parameters for understanding the response of the system to the presence of oxygen, assuming diffusion controlled quenching, are the unquenched lifetime of the dye ($\tau°$) and the diffusion coefficient (D_{O2}) and solubility (S_{O2}) of oxygen in the polymer matrix.

One can imagine many ways in which the presence of filler particles in an oxygen-sensor matrix can influence the behavior of the system. First, the dyes may adsorb onto the surface of the particles. Thus, the particles can affect the distribution of dye molecules in the film. Second, the particles can act as obstacles for oxygen diffusion: At particle concentrations of only a few volume percent, for triplet sensors, the mean separation between the particles can be much smaller than the mean diffusion length of oxygen during the time defined by the excited-state lifetime of the dye. Thus, the diffusion pathway for oxygen molecules becomes much more tortuous than in the absence of filler. Third, depending upon the nature of the polymer interaction with the particle surface, the particles can reduce or enhance the local free volume of the polymer matrix in the vicinity of the particle−polymer boundary.[7] This effect would reduce or enhance, respectively, the local diffusion rate of oxygen in these domains. Finally, oxygen can adsorb to the filler particles[8] and diffuse along this surface.[9] Thus, the particles may provide a new pathway for oxygen transport in the matrix. The magnitude of these various contributions is likely to be affected by the state of aggregation of the filler particles in the composite film.

In this paper, we describe experiments that examine the influence of silica as a filler on the performance of two types of polymer films employed as oxygen sensors. In an attempt to sort out some of the factors described in the preceding paragraph, we have chosen to compare two model systems involving a common dye. The dye, platinum octaethylporphine (PtOEP), with a phosphorescence lifetime on the order of 100 μs, was chosen because it exhibits clean exponential decay profiles in

10.1021/ma001454j CCC: $20.00
Published on Web 03/06/2001

both polymers of interest, poly(dimethyl siloxane) (PDMS) and poly(*n*-butylamino thionylphosphazene) (C_4PATP). We chose linear polymers to avoid problems that might arise due to cross-linking in polymer networks. The silica particles used as the filler were obtained as monodisperse hard spheres, 10 nm in diameter, dispersed in an organic solvent. By preparing films from a solution containing the dye, the polymer, and the colloidal dispersion of the silica particles, we minimize the tendency for the particles to aggregate during film formation.

We are particularly interested in using this dye particle−polymer combination for monitoring surface air-pressure profiles for objects in wind tunnels, a technique known as "phosphorescence barometry."[10−14] In this technique, an object (a model airplane or wing, a turbine blade, or an automobile) coated with an oxygen-sensing polymer coating ("pressure-sensitive paint," PSP) is examined in a wind tunnel. The object is illuminated with light of an appropriate wavelength to excite the dye, and the luminescence profile from the object is monitored with a digital camera. From the intensity of the dye at each pixel, one calculates the local surface air-pressure, and these data are combined to obtain a surface-pressure profile across the object. The proper connection between the dye intensity at each pixel and the surface air pressure depends on an understanding of the relationship between the partial pressure of oxygen at the surface of the film and the kinetics of dye quenching by oxygen molecules within the film.

Linear C_4PATP and its derivatives have shown some success in PSP applications.[15,16] In wind tunnel tests, C_4PATP does not appear to suffer serious abrasion, but it does tend to get covered with dust that sticks to the surface. Linear high-molecular-weight PDMS is too fluid to serve as a useful PSP. Composite films of both polymers containing 10−16 vol % silica have improved mechanical properties for this application, with little or no tack and no tendency to flow when exposed to wind at high velocities. To examine the influence of the silica particles on oxygen diffusion and oxygen permeation in these films, we carried out both time-scan and pulsed-laser experiments as a function of silica content on films containing PtOEP. To assess the location of the dye in these samples, we examined the absorption and emission spectroscopy of the dye. These experiments indicate a different location for the dye in the two polymers. In PDMS, the dye molecules adsorb to the surface of the silica particles. In C_4PATP, the dyes do not adsorb but remain dissolved in the polymer medium.

2. Experimental Section

2.1. Materials. PDMS was purchased from Polyscience, Inc. (Washington, PA). This sample is a linear polymer with a vendor-reported molecule weight of 500 000. It is a gel-like solid with a reported viscosity of 2 500 000 cSt (25 °C). It was used as received. Poly(*n*-butylamino thionylphosphazene), with a glass-transition temperature (T_g) of − 16 °C[16] is the same sample reported previously.[15] Its molecular weight, based upon gel permeation chromatography measurements with polystyrene standards, is $M_w = 1.6 \times 10^5$ and $M_w/M_n = 2.29$. Silica nanospheres were obtained as a 30 wt % dispersion in methyl isobutyl ketone (MIBK) from Nissan Chemical Ind., Ltd. (Tokyo, Japan). The particles are reported by the company to be nonporous and with a narrow size distribution and a diameter of 10 nm. Platinum octaethylporphine (PtOEP) was purchased from Porphyrin Products Inc., Logan, UT, and was used without further purification. The structure of the polymers we examine and of the dye PtOEP are shown in Scheme 1.

Scheme 1

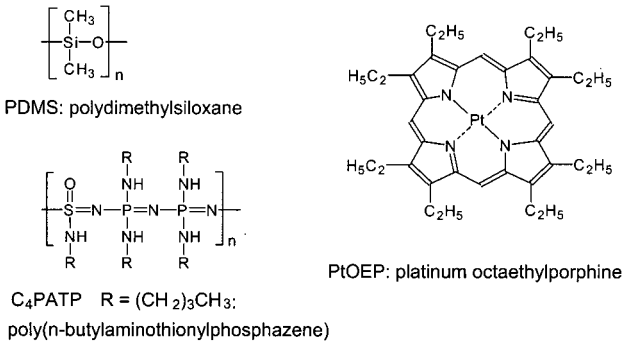

2.2. Preparation of Polymer-Silica Films Containing the Luminescent Dye. Polymer solutions were prepared consisting of 0.5 g of polymer (PDMS or C_4PATP) and 0.05 mg of the PtOEP dissolved in 10 mL of methyl isobutyl ketone (MIBK). To these solutions, measured amounts of 30 wt % of the silica/MIBK dispersion were added at room temperature. After this mixture was stirred for half an hour, an aliquot was cast onto a cut glass microscope slide (2.0 cm × 1.3 cm × 0.1 cm). Those slides were placed in a covered container with a small opening in order to slow the rate of solvent evaporation. The container was stored in the dark at room temperature. The films on the slides became hard to the touch after 1 day of drying and were then moved to an oven. They were heated at 60 ± 1 °C at ambient pressure for 24 h, followed by annealing at 60 °C under vacuum (<1 Torr) for 48 h. With this procedure, we can remove solvent from sample films without creating voids or air bubbles. The coated glass slides were then allowed to cool to room temperature. The thickness of the polymer film was determined by measuring the thickness of the film on the substrate with a Mitutoyo thickness gauge and then subtracting the thickness of the glass substrate. The films we examined ranged in thickness from 50 to 250 μm. Silica content in volume percent was calculated using literature density values of 2.2 g/cm^3 for silica[17] and 0.97 g/cm^3 for PDMS.[17] In the absence of a measured value for C_4PATP, we assume that its bulk density is ca. 1.0 g/cm^3. With an Abbe refractometer, we measured the refractive index (n_D) for our PDMS (1.4050) and C_4PATP (1.5053) samples.

2.3. Time-Scan Measurements. Time-scan measurements were carried out using a SPEX fluorolog 2 spectrometer equipped with a DMA 3000 data system. In such an experiment, the glass substrate supporting the polymer film was mounted in a cell (4.0 cm × 1.0 cm × 1.0 cm) that allows control of the surrounding atmosphere inside the sample chamber. The cell was flushed with nitrogen until virtually all of the oxygen was removed from the film as noted by the constant luminescence emission intensity (at its most intense value). At this point, the oxygen concentration was assumed to be zero both inside and outside of the film, and the emission intensity $I = I^o$ ($p_{O2} = 0$ atm). At time zero, the film was at once exposed to 1 atm air ($p_{O2} = 0.21$ atm). Inside the film, the oxygen concentration increases to its final uniform equilibrium value, and concurrently the measured emission intensity drops to its final value I_{eq}. This oxygen "diffusion-in" experiment is referred to an oxygen-sorption experiment. The same sample film is now ready for an oxygen-desorption experiment. That is, the external pressure of oxygen was at once brought to zero by flushing the cell with nitrogen. There is a net diffusion of quenchers (oxygen) out of the sample, until the oxygen concentration is nearly zero everywhere in the film. The measured intensity concurrently increased from I_{eq} to I^o.

The luminescence measurement was performed in the front-face geometry and the slits for light beams were set between 0.5 and 1.5 mm depending on the thickness of the film used. All spectra were recorded in the S/R (source signal divided by reference signal) mode in 0.5 nm steps. For the linearity of response, the sample source signal was always kept less than

2×10^5 count s^{-1}. The volume of the cell holding the film−substrate were measured before and found to be 4 cm^3. The washout time for the gas (nitrogen or compressed air) was measured to be less than 0.1 s (when the gas pressure was set at 1 atm), so that we are assured of complete gas replacement in the cell within 0.1 s. This time period is much shorter than the monitoring time for an oxygen-sorption or -desorption experiment. All measurements were carried out at room temperature (22 ± 1 °C).

2.4. Pulsed-Laser Experiments. Lifetimes of PtOEP phosphorescence in the absence of oxygen were measured in the pulsed-laser experiments by using the second harmonic of a Nd:YAG laser (Spectra Physics DCR 2) at 532 nm with a pulse width of 10 ns as the excitation source. The beam intensity was severely attenuated to prevent sample damage and dye photobleaching. Following sample excitation, the phosphorescence of the polymer films was detected by a Hammamatsu 956 photomultiplier tube connected to a Tektronix model 1912 transient digitizer. The decay trace was then transferred to a PC-type computer for analysis. Two types of filters were used here: a BP 510−610 nm band-pass filter (Balzers K-55) for the excitation beam and a BBP 650 nm broad-band-pass filter (Balzers K-65) for the emission beam.

3.Theoretical Consideration

Detailed descriptions of the theories of oxygen quenching and the methodology for determining the oxygen diffusivity, solubility, and permeability by time-scan and pulsed-laser experiments are presented in previous publications.[16,19] Here we summarized the concepts and key equations for data analysis.

In a luminescence quenching experiment, a luminescent dye is excited with either a pulse of light or with steady illumination. In the absence of oxygen or any other added quencher, the excited dye will decay with its unquenched lifetime τ^o. When a mobile quencher, such as oxygen, is present, the interaction of the excited dye with the quencher leads to the deactivation of the excited state. Dynamic quenching normally follows the Stern−Volmer (SV) equation, which expresses the relationship between the luminescence intensity (or lifetime) and quencher concentration.

$$\frac{I^o}{I} = \frac{\tau^o}{\tau} = 1 + k_q \tau^o [Q]_{eq} \tag{1}$$

In this expression, I is the emission intensity at some molar quencher concentration [Q], and I^o is the corresponding intensity in the absence of quencher. The derivation of eq 1 assumes that the relaxation of the solvent around the excited dye and the redistribution of reactants in the solution are faster than the reaction itself; i.e., the concentration of Q in the solution is effectively uniform, and the radial distribution function of Q surrounding each excited dye molecule is uniform. As a consequence, the decay of the electronically excited dye follows first-order kinetics in the absence of Q and pseudo-first-order kinetics in the presence of Q. In other words, the excited dye molecule exhibits an exponential decay profile, with lifetime τ^o in the absence of Q, and τ in its presence.

The rate coefficient k_q is related to the diffusivity of the quencher. For fluid media,

$$k_q = \alpha k_{diff} \tag{2}$$

where α is the probability of quenching in an encounter complex of the excited state/quencher and k_{diff} is the diffusion-controlled rate constant for the formation of the encounter pair. The diffusional encounter theory of Smoluchowski provides a direct proportionality relation between the steady-state value of k_{diff} and the quencher diffusion coefficient D_Q (where $D_Q = D_{O2} + D_{dye}$).

$$k_{diff} = 4\pi\sigma N_A' D_Q \tag{3}$$

In this expression, σ is the sum of the radii of the diffusing species, normally taken to be the interaction distance in the encounter complex (about 1 nm), and N_A' is 10^{-3} × Avogadro's number. Since $D_{O2} \gg D_{dye}$, one normally sets $D_Q = D_{O2}$. Substituting eqs 2 and 3 into eq 1 yields

$$\frac{I^o}{I} = \frac{\tau^o}{\tau} = 1 + (4\pi\sigma\alpha N_A' \tau^o D_Q)[Q] \tag{4a}$$

The parameter $B = (I^o/I_{eq} - 1)$ is defined as a measure of the response of the system at equilibrium upon exposure to air. When the final equilibrium state is 1 atm air (0.21 atm oxygen),

$$B = (4\pi\sigma\alpha N_A' \tau^o D_Q)[Q]_{0.21\ atm} \tag{5}$$

It is important to recognize that B contains the product $\sigma\alpha$, which can be thought of as an effective encounter radius. While much has been written about α, and how it differs for singlet quenching compared to triplet quenching, it is common to assume that quenchers such as oxygen have efficiencies α near unity and collision radii σ around 1.0 nm.[19−21]

During the approach to equilibrium, the oxygen concentration [Q] is not uniform through the polymer film. If the oxygen diffusion obeys Fick's second law, then the diffusion equation must be integrated in a way that takes proper account of the boundary conditions at the surfaces of the film. For a film on an impermeable substrate, the oxygen concentration in a layer at a distance x away from the gas/film interface at time t is given by the following expressions

Oxygen Sorption:

$$[Q](x, t) = [Q]_{0.21atm}\left[1 - \frac{4}{\pi}\sum_{n=odd}^{\infty}\frac{1}{n}\exp\left\{-\frac{n^2\pi^2 D_{O2} t}{4L^2}\right\} \times \sin\left(\frac{n\pi x}{2L}\right)\right] \tag{6a}$$

Oxygen Desorption:

$$[Q](x, t) = [Q]_{0.21atm}\left[\frac{4}{\pi}\sum_{n=odd}^{\infty}\frac{1}{n}\exp\left\{-\frac{n^2\pi^2 D_{O2} t}{4L^2}\right\} \times \sin\left(\frac{n\pi x}{2L}\right)\right] \tag{6b}$$

Within a thin layer, the oxygen concentration is effectively constant. The intensity of the light emitted from this layer can be described by a Stern−Volmer-type expression

$$\frac{\delta I^o}{\delta I(x, t)} = 1 + \frac{B[Q](x, t)}{[Q]_{0.21atm}}; \quad \delta I^o = I^o dx/L \tag{7}$$

where L is the thickness of the film. The intensity of light emitted from the entire film at time t is given by

the summation over the layers in the film:

$$I(t) = \frac{I^o}{L}\int_0^L \frac{dx}{1 + B[Q](x, t)/[Q]_{0.21atm}} \quad (8)$$

If both D_{O2} and L are known, one can replace the $[Q](x, t)$ term in eq 7 by eq 6, and then integrate it to calculate the time profile of the emission intensity of the film. The result of this calculation is a *simulated* intensity versus time profile, calculated with measured values of B and L and arbitrarily chosen values of D_{O2}. The diffusion coefficient is treated as an adjustable parameter in comparing simulated $I(t)$ profiles with those measured experimentally. The best fit is obtained by a minimization of the statistical parameter χ^2.

In terms of the external oxygen partial pressure p_{O2} (0.21 atm), the equilibrium solubility $[Q]_{eq}$ is proportional to p_{O2} in the range of low to moderate pressure, according to Henry's law, $[Q]_{eq} = S_{O2}p_{O2}$. In this equation, S_{O2} is the Henry's law constant of the gas solubility. When oxygen acts as quencher, eq 5 can be rewritten as

$$B = 4\pi\alpha\sigma N_A'\tau^o(S_{O2}D_{O2})p_{O2} \quad (9)$$

where the product of S_{O2} and D_{O2} is the oxygen permeability, P_{O2}.

The permeability P_{O2} can also be calculated from luminescence decay measurements, which are carried out on the polymer film in equilibrium with various partial pressures of oxygen. We have rewritten part a of eq 4 as part b to emphasize the predicted linear dependence of the lifetime ratio τ^o/τ versus p_{O2}. The slope of that plot should be equal to $4\pi N_A'\alpha\sigma\tau^o P_{O2}$. Implicit in this analysis is the assumption that the decay profile of the excited dye in the polymer matrix is exponential.

$$\frac{\tau^o}{\tau} = 1 + 4\pi N_A'\alpha\sigma\tau^o(D_{O2}S_{O2})p_{O2} \quad (4b)$$

4. Results

The silica particles we employ have their surface modified to provide colloidal stability in organic solvents such as MIBK. As a consequence, it is straightforward to prepare solutions of the polymers PDMS or C_4PATP in MIBK + silica without aggregation of the silica particles. The features of the particle surface, which promote colloidal stability in the solvent, may not operate as well in the bulk polymer. With the introduction of the 10 nm silica nanospheres into the polymer films, the films became harder to the touch. The increase in film hardness is the classic "filler effect" referred to in the Introduction. The maximum amount of filler that can be accommodated in a polymer films while maintaining the polymer as the continuous phase is referred to as the critical pigment volume composition (CPVC).[22] Pigment content greater than the CPVC results in air voids in the composite. In all of our experiments, the amount of silica added is well below the CPVC.

4.1. PDMS−Silica. The silica-free PDMS films are colorless, soft, and transparent. With the introduction of the silica nanospheres into the PDMS films, the films became harder, and the hardness increased with silica content. PDMS films containing significant amounts (e.g., >10 wt %) silica are hazy, but not opaque.

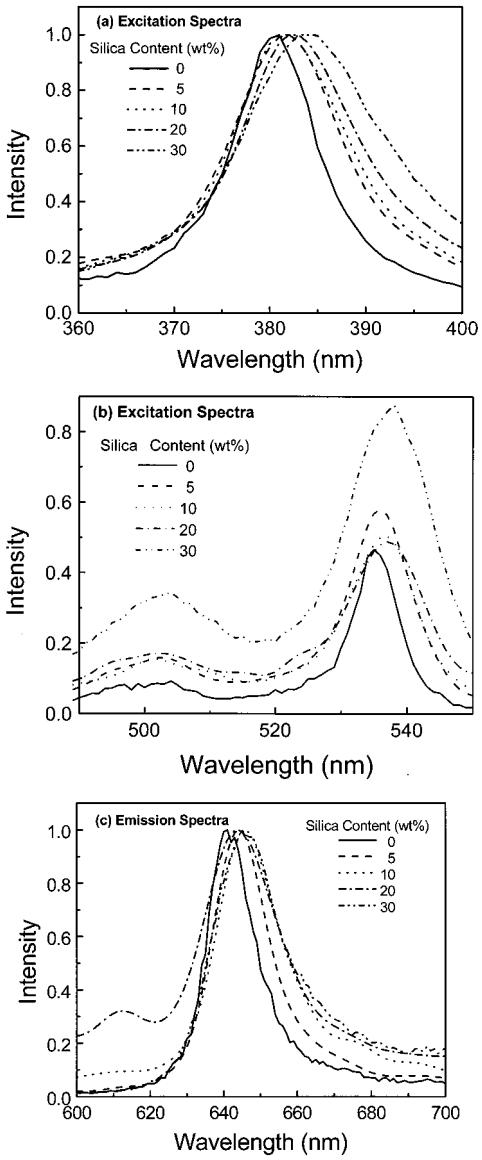

Figure 1. Normalized photoluminescence spectra of PtOEP in silica-free and -filled PDMS films in a nitrogen environment: (a) first part of excitation spectra (360−400 nm), λ_{em} = 641 nm; (b) second part of excitation spectra (490−550 nm), λ_{em} = 641 nm; and (c) emission spectra, λ_{ex} = 534 nm.

Photoluminescence Spectra. Parts a and b of Figure 1 show the excitation spectra of PtOEP in PDMS in the presence and absence of silica, respectively. The Soret band at 381 nm in the silica-free sample is redshifted progressively with increasing silica, and the maximum appears at 383 nm in the sample with 30 wt % silica (in Figure 1a). A similar shift is seen in the low-energy band at 534 nm for the silica-free film shown in Figure 1b. The changes in intensity seen with increasing silica content for these films of similar thickness and dye content are a consequence of an increase in light scattering caused by the silica. In Figure 1c, we show the corresponding fluorescence spectra. In the presence of silica, the peak position shifts from 640 to about 645 nm, and the band is broadened significantly.

Time-Scan Measurements. PDMS has a very low T_g (−120 °C) and high oxygen permeability and diffusivity.[23] To establish a baseline for our experiments with silica, we first examine a PDMS film in the absence of added pigment. The results of time-scan experiments for a silica-free PDMS film containing 100 ppm PtOEP

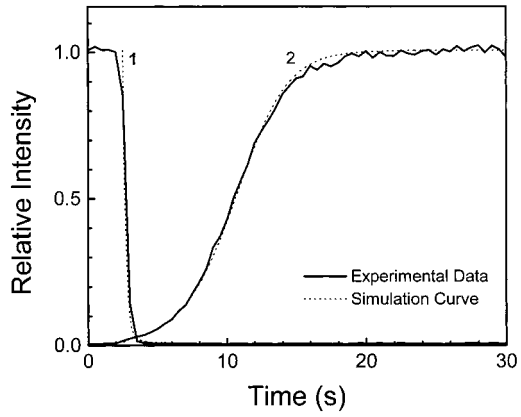

Figure 2. Plots of the luminescent intensity of PtOEP (100 ppm) in a film of silica-free PDMS ($L = 0.116$ mm) on glass as a function of time. The emission is observed at 645 nm during steady-state excitation at 535 nm. Curve 1 ($D_{O2} = 2.30 \times 10^{-5}$ cm^2 s^{-1}) is obtained from an oxygen sorption experiment; curve 2 ($D_{O2} = 2.25 \times 10^{-5}$ cm^2 s^{-1}) is from an oxygen desorption experiment.

Table 1. Parameters of Oxygen Diffusion and Permeation in Silica-Filled and Unfilled PDMS Films

silica (wt %)	B ($I^o/I_{eq} - 1$)	$\langle\tau\rangle^o$ (μs)	$10^5\ D_{O2}$[a]	$10^{12}\ P_{O2}$[a] (from B)
0	176 ± 16	65 ± 4	2.22 ± 0.23	18 ± 2[b]
5	45 ± 8	78 ± 1	1.84 ± 0.20	3.8 ± 0.7
10	30 ± 4	84 ± 2	1.79 ± 0.11	2.4 ± 0.3
20	11 ± 3	96 ± 2	1.72 ± 0.15	0.76 ± 0.21
30	9 ± 3	91 ± 1	1.44 ± 0.16	0.65 ± 0.22

[a] Units: D, cm^2 s^{-1}; P, mol cm^{-1} s^{-1} atm^{-1}. [b] For PDMS in the absence of silica, $S_{O2} = 8.2 \pm 1.1 \times 10^{-4}$ M atm^{-1}

is shown in Figure 2. During oxygen sorption (curve 1), the emission intensity drops rapidly. In contrast, the intensity increases at a much slower rate during oxygen desorption (curve 2). Although the intensity−time profiles are quite different, they both fit well to the Fickian diffusion model as described by eq 6 and 8. The best-fit D_{O2} values for both experiments are essentially identical: $D_{O2} = 2.30 \times 10^{-5}$ cm^2 s^{-1} for oxygen-sorption and $D_{O2} = 2.25 \times 10^{-5}$ cm^2 s^{-1} for oxygen-desorption. These results confirm that the oxygen diffusivity in both experiments is the same. The difference in the shape of the sorption and desorption profiles is related to the way in which the quenching kinetics, eq 8, couples with the Fickian diffusion of the quencher, eq 6. The average D_{O2} value obtained from 12 measurements on four PDMS samples with various thicknesses is $D_{O2} = 2.22 \pm 0.23 \times 10^{-5}$ cm^2 s^{-1}. The value of P_{O2} (18×10^{-12} mol cm^{-1} s^{-1} atm^{-1}) and S_{O2} (8.2×10^{-4} M atm^{-1}) are calculated using the D_{O2} and B values (Table 1).In Figure 3, we plot the results of time-scan experiments carried out on a PDMS film containing 30 wt % silica. This film has the same dye concentration as that in Figure 2. The curves are similar to those of the silica-free PDMS films: the rate of intensity increase during oxygen-desorption (curve 2) is slower than the rate of intensity decrease during oxygen-sorption (curve 1). The oxygen diffusion coefficients (D_{O2}) calculated from both curves, are very close: i.e., 1.50×10^{-5} cm^2 s^{-1} for oxygen sorption and 1.66×10^{-5} cm^2 s^{-1} for oxygen desorption. These D_{O2} values are only about 25% smaller than those for the silica-free PDMS films. More pronounced, however, is the decrease in the value of B ($=I^o/I_{eq} - 1$), from 176 for PDMS to 9 for PDMS−silica (30 wt %). It is important to emphasize that B values are determined

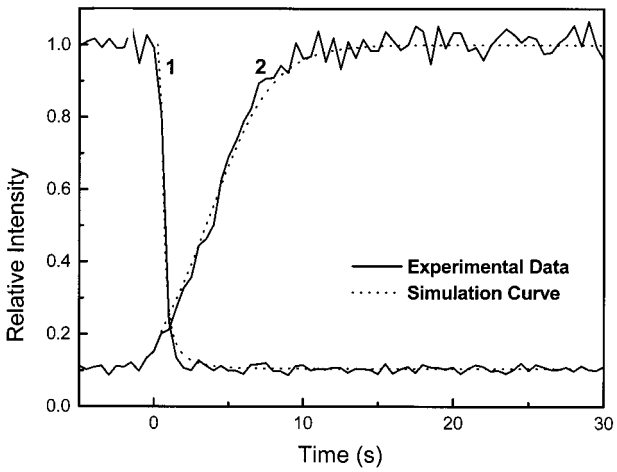

Figure 3. Plots of the luminescent intensity of PtOEP (100 ppm) in a film of PDMS−silica (30 wt %, $L = 0.090$ mm) on glass as a function of time. The emission is observed at 645 nm during steady-state excitation at 535 nm. Curve 1 ($D_{O2} = 1.50 \times 10^{-5}$ cm^2 s^{-1}) is obtained from an oxygen sorption experiment; curve 2 ($D_{O2} = 1.66 \times 10^{-5}$ cm^2 s^{-1}) is from an oxygen desorption experiment.

independent of the diffusion coefficients, D_{O2}. B values are calculated from the ratio of emission intensities ($I^o/I_{eq} - 1$) of equilibrium states of the film. D_{O2} values are determined from the rate at which the system approaches equilibrium upon a change in the external partial pressure of oxygen.

Similar experiments were carried out on other samples of PDMS containing various amounts of silica. The values of D_{O2} and P_{O2} from these experiments are collected in Table 1. In Table 1 we see that the B values decrease dramatically as the silica content is increased: i.e., a decrease from 176 ± 16 (PDMS) to 9 ± 3 (PDMS−silica (30 wt %)) by a factor of 18. Both D_{O2} and P_{O2} values decrease with an increase of silica concentration, but the decreases in the calculated values of P_{O2} are much more pronounced, reflecting the changes in B.

Unquenched Lifetime. Under pulsed laser excitation, the PtOEP/PDMS film examined in the absence of oxygen exhibits an exponential decay. In comparison, the decay of PtOEP in PDMS−silica (10 wt %) is nonexponential in the absence of oxygen, and the decays show a much more obvious curvature when the p_{O2} is increased. For nonexponential decays, we calculate mean decay times $\langle\tau\rangle$ (see eq 10 below). Values of the unquenched lifetimes of silica-free (τ^o) and -filled ($\langle\tau\rangle^o$) PDMS films are listed in Table 1. Values of $\langle\tau\rangle^o$ increase from 65 to 90 μs as the silica content is raised from 0 to 30 wt %.

4.2. C_4PATP−Silica. C_4PATP itself forms light yellow films, which are soft and tacky. Silica-filled C_4PATP films become harder, and the tackiness of the film surface disappears when the silica fraction is increased to greater than 20 wt %. These films remain transparent for all levels of silica incorporation examined here.

Photoluminescence Spectra. The excitation spectra of PtOEP in C_4PATP films are shown in parts a and b of Figure 4. In Figure 4a, we see that the maximum of the Soret band appears at 383 nm. The presence of substantial amounts of silica lead to apparent band broadening, especially on the low wavelength side of the peak. In Figure 4b, we find that the presence of silica has almost no effect on the position of the low energy band

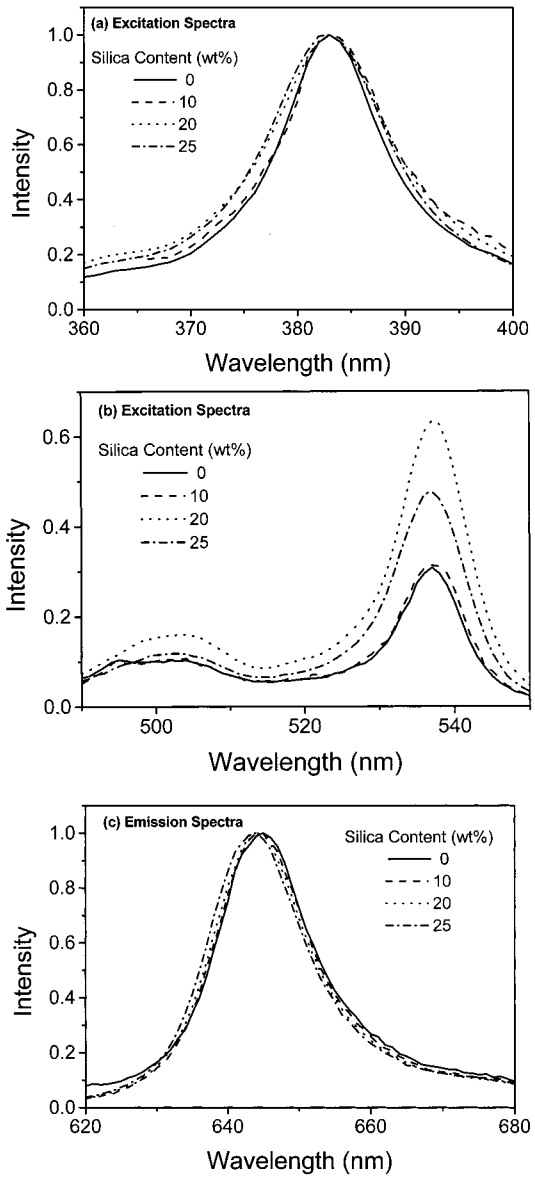

Figure 4. Normalized photoluminescence spectra of PtOEP in silica-free and -filled C_4PATP films in a nitrogen environment: (a) first part of excitation spectra (360−400 nm), λ_{em} = 645 nm; (b) second part of excitation spectra (490−550 nm), λ_{em} = 645 nm; and (c) emission spectra, λ_{ex} = 535 nm.

at 535 nm. The increase in intensity for the films with higher silica content is due in part to an increase in light scattering caused by the silica. The corresponding emission spectra are presented in Figure 4c. In the absence of silica, the peak appears at 643 nm, redshifted by about 3 nm from the emission peak for this dye in PDMS. When silica is present, there are almost no changes in the shape of the emission band and a very small blueshift of the peak maximum.

Time-Scan Measurements. In previous reports,[16] we described oxygen diffusion and oxygen permeation measurements on C_4PATP. As in the case of PDMS, quenching of dye phosphorescence in C_4PATP is completely consistent with eqs 4, 8, and 9. We have repeated these experiments here (Figure 5, curve 1 for oxygen sorption and curve 2 for oxygen desorption) in order to establish a baseline to compare with silica-filled C_4PATP films. For several PtOEP/C_4PATP films, we obtain an average of $D_{O2} = 3.73 \times 10^{-6}$ cm^2 s^{-1} for both oxygen sorption and -desorption experiments. The values of P_{O2},

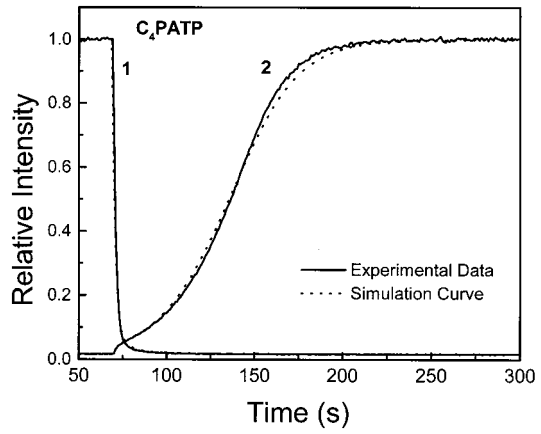

Figure 5. Plots of the luminescent intensity of PtOEP (500 ppm) in a film of silica-free C_4PATP (L = 0.125 mm) on glass as a function of time. The emission is observed at 645 nm during steady-state excitation at 535 nm. Curve 1 ($D_{O2} = 3.28 \times 10^{-6}$ cm^2 s^{-1}) is obtained from an oxygen sorption experiment; curve 2 ($D_{O2} = 3.58 \times 10^{-6}$ cm^2 s^{-1}) is from an oxygen desorption experiment.

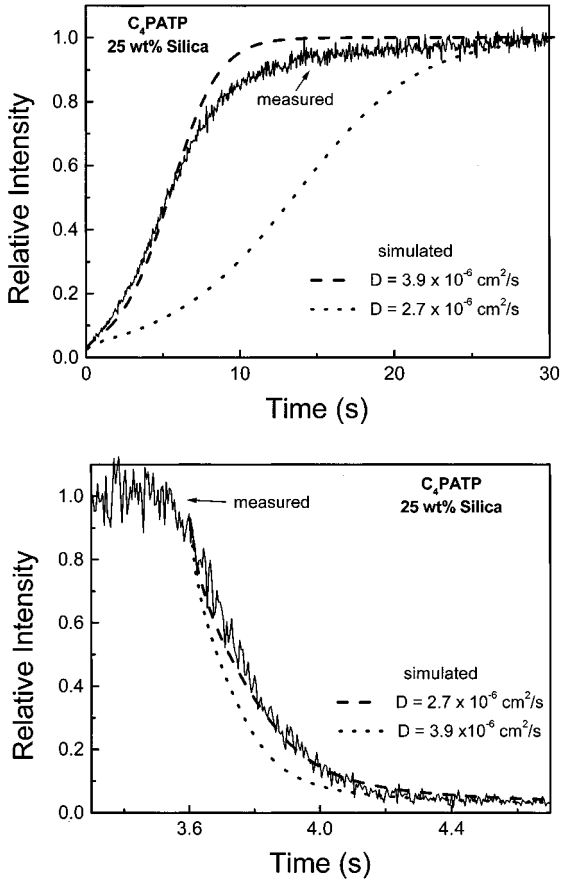

Figure 6. Plot of the luminescent intensity of PtOEP (600 ppm) in a film of C_4PATP−silica (25 wt %, L = 0.043 mm) on glass as a function of time. The emission is observed at 645 nm during steady-state excitation at 535 nm. (a: top) Oxygen desorption intensity profile. (b: bottom) Oxygen sorption intensity profile.

which are calculated from the value of B and from the lifetime Stern−Volmer plot (cf., eq 4) are rather close (from B, $P_{O2} = 3.85 \times 10^{-12}$ mol cm^{-1} s^{-1} atm^{-1}; from the plot of τ^o/τ, $P_{O2} = 4.03 \times 10^{-12}$ mol cm^{-1} s^{-1} atm^{-1}).

In parts a and b of Figure 6,we present the results of the corresponding oxygen-desorption and -sorption experiments for a film of C_4PATP−silica containing 25 wt

Table 2. Parameters of Oxygen Diffusion and Permeation in Silica-Filled and Unfilled C_4PATP Films

silica (wt %)	B ($I^o/I_{eq} - 1$)	τ^o (μs)	$10^6\ D_{O2}$[a]	$10^{12}\ P_{O2}$[a] (from B)
0	60 ± 4	102.4 ± 0.4	3.7 ± 1.0	3.9 ± 0.4
10	55 ± 2	104.0 ± 0.1	3.0 ± 0.6[b] 5.3 ± 1.0[c]	3.5 ± 0.3
20	49 ± 3	104.5 ± 0.5	3.0 ± 0.8[b] 4.8 ± 0.5[c]	3.1 ± 0.3
25	50 ± 4	104.7 ± 0.3	2.7 ± 0.9[b] 3.9 ± 0.9[c]	3.2 ± 0.2

[a] Units as in Table 1, footnote a. [b] Diffusion coefficients obtained by fitting the oxygen-sorption intensity profiles. [c] Apparent diffusion coefficients obtained from the simulated intensity growth profile that best fits the data up to the midpoint of the oxygen-desorption experiments.

% silica. In Figure 6a, we see that the emission intensity starts to increase rapidly when oxygen is flushed from the cell, and the growth in intensity becomes slower as the film approaches equilibrium with the nitrogen atmosphere. Unlike the silica-free C_4PATP film, the presence of silica causes a deviation between the experimental profile and the simulated data curve, especially for times after the "midpoint" in the intensity profile, when the intensity is equal to $(I^o + I_{eq})/2$. For the sample containing 25 wt % (ca. 16 vol %) silica, we can fit the first half of the recovery curve reasonably, but the later stages of the diffusion process take longer than expected from a Fickian model based upon a single diffusion coefficient for oxygen. This simulated curve is based upon an assumed value of $D_{O2} = 3.9 \times 10^{-6}$ cm^2 s^{-1}, which we will call an "apparent diffusion coefficient." The value of D_{O2} calculated by fitting the data up to the midpoint gives a value representative of the most mobile oxygen molecules in the system. Apparent diffusion coefficients calculated in this way for all of the C_4PATP films are collected in Table 2.In Figure 6b, we present an example of the oxygen-sorption plot. The samples used in Figure 6a,b are the same, but the situation here is more complicated. When we fit the experimental data to the theoretical model for oxygen sorption (eqs 6a and 8), the best fit gives a value of $D_{O2} = 2.7 \times 10^{-6}$ cm^2/s. This value of oxygen diffusivity is lower than the apparent diffusion coefficient in the oxygen-desorption experiment (3.9×10^{-6} cm^2/s). In Figure 6b, we also plot another simulated curve, which is obtained by assuming D_{O2} equal to 3.9×10^{-6} cm^2/s. However, the curve simulated with this apparent diffusion coefficient decays more rapidly than the experimental curve. The difference between the two simulated curves in Figure 6b is not large. If we return to the oxygen desorption experiment in Figure 6a, we see that the smaller D_{O2} value gives a simulated curve that does not correspond at all to the experimental result.

Unquenched Lifetime. In the absence of oxygen, the decays of the excited dye in both silica-free and -filled C_4PATP films systems are exponential, and their unquenched lifetimes are very close: 102 μs for C_4PATP films and 104 μs for C_4PATP−silica films. This result indicates that in the absence of oxygen, the decay profiles of PtOEP in C_4PATP films appeared to be independent of the amount of silica present (Table 2).

5. Discussion

Film Properties. Early experiments on silica-filled PDMS films showed that air voids were present in the films if the films were dried too rapidly. We therefore developed a protocol involving slow solvent evaporation (over 56 h) followed by heating the sample to 60 °C for 24 h and only then heating the film under vacuum. In this way, bubbles in the films could be avoided. For C_4-PATP, there was a smaller propensity for bubble formation. Void-free films could be obtained by drying the films over 24 h in the open air, followed by the annealing and vacuum-oven steps. As the amount of silica in the films was increased, the films became firmer to the touch and less tacky. Films containing 20 wt % or more silica were essentially tack-free for both PDMS and for C_4PATP.

All PDMS films containing more than 10 wt % silica (4.7 vol %) were hazy. No voids or silica aggregates could be observed with an optical microscope. Turbidity depends on the magnitude of the difference in refractive index between the particles and the matrix, as well as on the size of the objects which scatter light. The haziness of the PDMS films suggests that there may be some tendency for silica to form small aggregates in PDMS. These aggregates, if present, are too small to observe by optical microscopy. In contrast, films containing up to 25 wt % silica in C_4PAPT are transparent.

Location of the Dye. The unquenched luminescence decay profile of PtOEP is exponential in both PDMS and C_4PATP films. This result is a strong indication that there is no dye aggregation in these films at the dye concentrations employed and that all dye molecules experience essentially identical environments during their excited-state lifetime.

The redshifts of the excitation and emission spectra of PtOEP in PDMS−silica composite films, in comparison with the PDMS films themselves, indicate that the environment of the PtOEP molecules is affected by the presence of the silica nanospheres. This effect is probably due to the adsorption of PtOEP molecules on the surface of the silica particles combined with the formation of dye aggregates. Aggregation accompanying adsorption of dyes on inorganic particles such as silica and alumina is well-known.[24] Costa's group has examined porphyrin adsorption onto silica,[25] eosin adsorption onto alumina,[26] and the effects of this adsorption on the quenching of triplet states by oxygen. For the case of eosin adsorbed on powdered alumina, this group showed that adsorption took place at special sites so that aggregation was detected at only a tiny fraction of monolayer coverage. Springob and Wolff[27] examined the adsorption of fluoranthene onto silica gel from ethanol solution. They reported a shift in the excitation spectra of fluoranthene accompanying adsorption. As the surface coverage increased, an additional redshift was observed and was attributed to the formation of dye aggregates.

Demas et al.[3] took advantage of dye adsorption onto silica to create oxygen sensors. Their sensors are based on ionic ruthenium dyes that have poor intrinsic solubility in PDMS. In their system, the dyes are added to a curable silicone resin (RTV 118 from GE) that contains hydrophobized silica particles.[28] Klimant and Leiner have also designed oxygen sensors based on this combination and present evidence that the dyes in the matrix are adsorbed on the silica particles.[29]

When we add silica to PDMS films containing PtOEP, the unquenched decay profiles are no longer exponential. These decays were fitted to a sum of two or three

exponential terms. The mean decay time, defined as

$$\langle \tau \rangle = \frac{\sum_i A_i \tau_i}{\sum_i A_i} \qquad (10)$$

increases with increasing amounts of silica (Table 1). In a somewhat different system, Chu and Thomas[9b] found that dyes adsorbed to the untreated surface of silica particles in air exhibit a Gaussian distribution of lifetimes. Our data, including pulsed laser experiments that will be published separately,[30] indicate that a substantial fraction of the PtOEP dye molecules in PDMS are adsorbed to the silica and that adsorption of the dye leads to the formation of dimers and other larger dye aggregates. It is important to keep in mind that the silica we employ has its surface modified to make it dispersible in organic media. The driving force for dye aggregation on this surface is likely to be much less than that for the adsorption of dye onto bare silica or bare alumina.

Time-Scan Experiments and Oxygen Diffusion. Previous publications from our research group have shown that time-scan experiments for PtOEP in PDMS and in C_4PATP give results consistent with diffusion that satisfies Fick's Laws. Similar results are shown in Figures 2 and 5. When these experiments are repeated for films containing silica, we find excellent agreement for the PDMS films between the experimental intensity profiles and the simulated curves based on the assumption of Fickian diffusion (Figure 3). Even when the silica fraction reaches 30 wt % (16 vol %), little deviation from Fickian diffusion can be seen. These films have a pronounced haze. The decreased transparency leads to increased noise in the luminescence intensity profiles. What is remarkable about this result is that even though the dye is to a substantial extent adsorbed onto the surface of the silica particles, the dyes maintain their sensitivity to oxygen diffusion into the films in a way that is entirely consistent with Fick's Laws and a single-valued diffusion coefficient.

Similar experiments on C_4PATP films containing silica indicate that the behavior is more complicated. We can fit the intensity−recovery curves up to the midpoint with a single diffusion coefficient (Figure 6a), but there is a slower component to the diffusion of oxygen out of the film. It is ironic that silica-containing C_4PATP films, where the dye remains in the polymer phase, show more complex behavior than the PDMS−silica films, where we have strong evidence for dye adsorption to the silica particles.

The Silica Surface as a Reservoir for Oxygen. In this section, we develop a model to explain the seemingly simple behavior of PtOEP plus silica in PDMS, where most of the dye appears to be bound to the silica, and the more complex behavior of PtOEP−silica in C_4PATP, where the dye remains in the polymer matrix. This model is based on the idea that a significant fraction of oxygen in the film adsorbs to the surface of the silica particles. A picture describing this model is presented in Figure 7. In this figure, the term "O_2 in" refers to the oxygen sorption experiment, and "out" refers to a desorption experiment.

In the presence of air, for both silica-containing polymer films, oxygen is present in two distinct locations: dissolved in the polymer matrix and adsorbed to the silica surface. As suggested originally by Paul and Kemp[8a] and confirmed more recently by Kamiya et al.,[8c] we imagine that the presence of the silica particles does not perturb the solubility of gases like oxygen in the polymer itself. The O_2 molecules on the surface of the silica are free to diffuse across the surface and are in dynamic equilibrium with O_2 molecules in the matrix. In PDMS, since most of the dye molecules are also adsorbed to the silica particle surface, these dye molecules can be quenched by the surface-bound oxygen. In C_4PATP, the oxygen molecules at the silica surface are bound to a reservoir where they do not participate in the quenching process. From a spectroscopic view, PtOEP in C_4PATP is unaware of the oxygen bound to the silica surface.

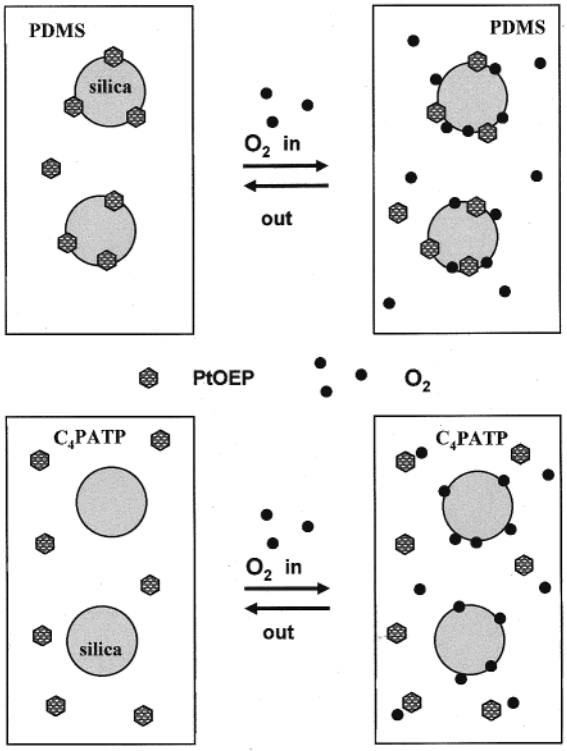

Figure 7. Model for the locus of dye and oxygen molecules in the two polymer films. The filled hexagons signify the PtOEP dye molecules, and the smaller filled circles represent O_2 molecules. In PDMS (top), almost all of the dye molecules are adsorbed to the surface of the 10 nm diameter silica filler particles. In C_4PATP, the dyes remain in the matrix. When oxygen is introduced into a system, it reaches its Henry Law solubility in the polymer matrix, and additional oxygen adsorbs to the particle surface. In PDMS, this bound oxygen can quench the excited dye molecules. In C_4PATP, the excited dyes in the matrix are unaware of additional O_2 adsorbed to the particle surface.

The key feature of this model is that the desorption rate of oxygen from the silica surface in C_4PATP is comparable to or somewhat slower than desorption of O_2 from the polymer into the atmosphere. In the early stages of a desorption experiment involving silica−C_4PATP, the excited dye molecules would sense a depleted oxygen concentration similar to that in the absence of silica. If oxygen desorption from the silica surface were relatively slow, it would add a slow component to the oxygen desorption kinetics. As this process takes place, these O_2 molecules maintain the oxygen concentration in the C_4PATP matrix at a higher level than would be the case if no silica were present.

The dye monitors a very different aspect of desorption of oxygen from the PDMS film containing silica. Since most of the dye is bound to the silica, desorption of oxygen from the silica leads to an immediate increase in the dye luminescence intensity. The fact that the desorption experiment for PDMS−silica appears to follow simple Fickian diffusion with a similar D_{O2} value as found in the oxygen sorption experiment suggests that in PDMS oxygen desorption from the silica surface is faster than the loss of oxygen from the PDMS matrix to the atmosphere.

For the process labeled "O_2 in," we find much smaller deviations from the simple Fickian diffusion model, for both PDMS (Figure 3) and C_4PATP films (Figure 6b) containing silica. We rationalize this result by imagining that oxygen adsorption onto the silica surface is diffusion-controlled. Fickian diffusion through the PDMS matrix controls the rate of quenching of dye molecules bound to the silica particles. In C_4PATP, quenching is rapid as oxygen first diffuses into the polymer film. The shape of the quenching curve is not much affected by the relatively small volume fraction (up to 16 vol %) of silica particles and the O_2 molecules that become bound to their surface.

Filler Effects on Oxygen Diffusion Rates. For PDMS−silica films, the values of D_{O2} calculated from the time-scan experiments are found to decrease slightly with an increasing volume fraction of silica in the matrix (see Table 1). The largest change is from 2.22×10^{-5} $cm^2\ s^{-1}$ for the silica-free PDMS film to 1.44×10^{-5} $cm^2\ s^{-1}$ for the film containing 30 wt % silica. While these changes are not large, they represent the influence of a small volume fraction of added particles.

Time-scan experiments are sensitive to oxygen on a length scale determined by the film thickness. The films we examined ranged in thickness from 50 to 250 μm. Each excited dye molecule, however, is sensitive to oxygen diffusion on a smaller length scale, determined by the mean diffusion distance of oxygen $(6D_{O2}\tau^o)^{0.5}$ during the excited-state lifetime of the dye. For C_4PATP, this diffusion distance is approximately 0.5 μm. For PDMS, it is about 1 μm. It is useful to compare this distance to the mean separation between silica particles in the matrix, assuming that the silica particles are not aggregated. For 10 vol % of 10 nm diameter particles, the mean interparticle distance is 17 nm. For 16 vol % silica, this distance is slightly smaller, 15 nm. Thus the mean diffusion distance of an O_2 molecule during the time τ^o is much larger than the mean separation between adjacent particles in the matrix.

Under these circumstances (see the drawing in Figure 8), the silica particles act as obstacles to increase the tortuosity of the path necessary for diffusion perpendicular to the film surface. Thus it takes a longer time for the solute to diffuse through the film. In the obstacle model, the local diffusion rate of oxygen in the matrix is unaffected by the presence of the obstacle, but the "measured" macroscopic diffusion coefficient is reduced in magnitude because of the increase in the diffusion path. Paul and Kemp[8a] review three different expressions that attempt to describe the effect of obstacles on reducing the rate of gas permeation in polymers. To describe the reduction in D_{O2} in our experiments, we employ the obstacle model of Mackie and Meares.[31,32] In this model, the experimental values of the diffusion coefficients of oxygen in the silica-free polymer, D_P, and in the silica-filled PDMS, $D_{P-silica}$, are related by the

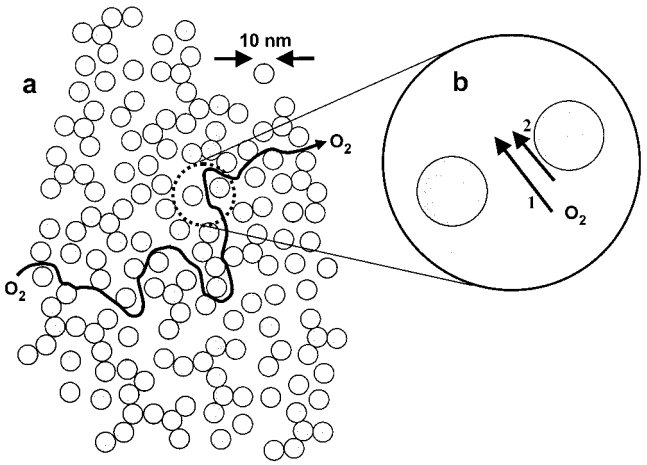

Figure 8. (a) Drawing indicating a diffusion path over 100 μs for an oxygen molecule in a polymer matrix containing 10 vol % of 10 nm hard spheres which do not aggregate or are only weakly aggregated. The mean diffusion length during the excited lifetime of the dye $\langle l^2\rangle^{1/2} = (6D_{O2}\tau^o)^{1/2}$ is equal to ca. 500 nm for O_2 in C_4PATP. (b) O_2 molecule diffusing along path 1 far from a particle surface diffusing at the same rate as that in pure polymer. A molecule diffusing close to the particle surface (path 2) would diffuse more slowly if the surface interacted strongly with the polymer matrix but more rapidly if the surface interacted only weakly with the polymer.

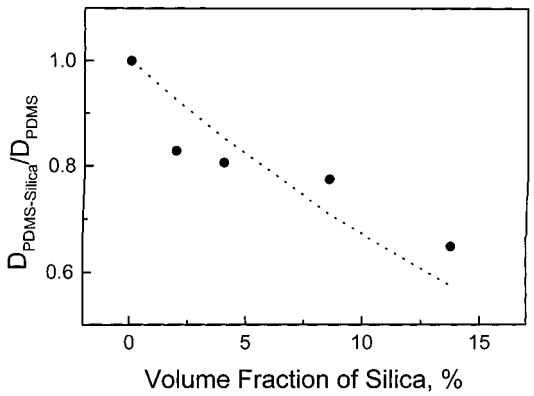

Figure 9. Effect of silica content on the oxygen diffusivity in PDMS films. The continuous curve (dotted line) describes the influence of obstacles on the diffusion rate and is calculated from eq 11.

expression

$$\frac{D_{P-silica}}{D_P} = \left[\frac{1-\phi_{silica}}{1+\phi_{silica}}\right]^2 \qquad (11)$$

where ϕ_{silica} is the volume fraction of silica nanospheres in the films. In Figure 9, we plot of the ratio of the diffusion coefficients determined for O_2 in PDMS against the volume fraction of silica and compare the results to that (the dotted line in Figure 9) calculated according to eq 11. There is scatter in the data, but the overall trend is consistent with the predictions of the obstacle model.

While the obstacle model explains the change in D_{O2} in PDMS as the silica particle content is increased, it does not explain the results in C_4PATP. The dotted line in Figure 9 predicts that 10 vol % silica in C_4PATP should lead to a 35% reduction in D_{O2}, and if silica does not affect the oxygen solubility in the polymer, it should have a similar effect on P_{O2}. We do not observe any such decrease in the values of D_{O2} and P_{O2} in C_4PATP. The

obstacle model also does not provide a complete description of our experimental observations for PDMS plus silica. In pulsed laser experiments, we observe that the luminescence decay profiles of PtOEP in PDMS plus silica exhibit a much stronger curvature in the presence of oxygen. This increase in curvature is suggestive of a distribution of oxygen mobilities in the system, reflecting an influence of the silica on polymer segment mobility in the vicinity of the particle surface. Thus other factors must also affect the diffusion rate of oxygen as sensed in our experiments.

To explain these differences between our results and the predictions of the obstacle model, we must speculate about the nature of the structures formed by the silica particles in the two polymers and the influence of these structures on oxygen diffusion. We know from optical microscopy that the silica particles do not form aggregates in either polymer large enough to be resolved. We observed that small quantities of silica (<10 vol %) were more effective in PDMS at reducing tack and increasing the stiffness than in C_4PATP. As a consequence, we imagine that silica forms open (fractal) aggregates in PDMS that percolate at lower volume fraction than that expected for hard spheres. The obstacle effect of open aggregates may not be very different than that predicted by eq 11.

If no large silica aggregates are formed in C_4PATP, there must be some second factor that increases the diffusion rate enough to compensate for the obstacle effect. Two possibilities come to mind. If C_4PATP interacts only weakly with the modified surface of the silica particles we employ, it is possible that rapid diffusion of oxygen on this surface could play a role. In addition, weakly interacting surfaces are thought to enhance the mobility of polymer segments near the surface.[7] This effect can lower the T_g of thin polymer films and enhance the diffusion rate of solutes such as oxygen through these domains. In Figure 8b, we imagine that O_2 molecules diffusing along path 1, far from a particle surface, diffuse at the same rate as in pure polymer. Molecules diffusing along path 2 diffuse more rapidly because of the enhanced mobility of the polymer chains near the weakly interacting surface.

Summary and Conclusions

We examined the influence of 10 nm diameter silica particles on oxygen diffusion and oxygen permeation in two different polymer films, PDMS and C_4PATP. The silica particles increase the modulus of the matrix and decrease the tackiness of the film. C_4PATP films are no longer tacky to the touch when the silica content reaches 30 wt % (16 vol %), close to the percolation threshold hard spheres. PDMS films lose their tack and become rigid at somewhat lower silica content (ca. 10 vol %). Silica aggregates with an open (fractal) structure can percolate at lower volume fractions than unaggregated hard spheres.

Luminescence experiments were carried out on films containing PtOEP as a sensor dye. We monitored the change in its phosphorescence intensity as oxygen was allowed to diffuse into or out of the film. In separate experiments, we measured the phosphorescence decay rate of the dye for films in equilibrium with a known external oxygen pressure. Spectroscopic studies of the dye absorption spectra, emission spectra, and luminescence decay profiles in PDMS showed that in this matrix a substantial fraction of the dye was adsorbed to the silica. Similar experiments showed that in C_4PATP, the dye remained almost entirely in the polymer phase.

Time-scan experiments on PDMS films showed that the quenching rate during oxygen sorption and the emission−intensity−recovery rate as oxygen diffused out of the film were completely consistent with Fickian diffusion, even in the presence of 30 wt % silica. Although most of the dye in this composite film is bound to the silica surface, the dynamic experiment is still sensitive to the rate of oxygen flux through the matrix. The diffusion coefficients decreased with increasing silica content, but the effect was rather small, with D_{O2} values decreasing from 2.2×10^{-5} cm^2 s^{-1} to 1.4×10^{-5} cm^2 s^{-1}. These small changes can be explained in terms of the silica particles acting as obstacles to oxygen diffusion.

Time-scan experiments on C_4PATP are complicated by the adsorption of oxygen onto the surface of the silica particles. In the sorption experiment, in which there is a rapid decrease in the dye emission intensity, one sees only a small effect of the silica particles. The experimental intensity−time profiles resemble the curves simulated with a single diffusion coefficient. For each experimental curve, the best-fit value of D_{O2} is close to that in the film without silica. More pronounced differences are seen in the desorption experiment, where there is a long tail in the plot of the growth of emission intensity versus diffusion time. We explain this result in terms of a model in which the silica particle surface acts as a reservoir for oxygen. As oxygen diffuses out of the C_4PATP matrix, it is replaced on a somewhat slower time-scale by oxygen desorbing from the surface of the silica particles. Oxygen permeability values P_{O2} can be calculated independently from the magnitude of B, which depends on the ratio of the dye emission intensity in films in equilibrium with an oxygen-free atmosphere and an air atmosphere. For C_4PATP films, the B values and P_{O2} values are unchanged by the presence of silica (Table 2). We conclude that dye molecules in this polymer are quenched by O_2 molecules in the matrix and are unaware of additional oxygen adsorbed to the surface of the silica particles. For PDMS, we obtain strange results as shown in Table 1. With increasing silica content, the B values decrease, even though the unquenched (mean) lifetime of PtOEP increases. By inference, P_{O2} values for this polymer decrease substantially, even though D_{O2} values decrease to a much smaller extent. If the model from which eqs 8 and 9 were derived continues to apply to PDMS−silica, we would reach the strange and unrealistic conclusion that introducing silica into a PDMS film lowers the oxygen solubility S_{O2} in the polymer matrix. At present, we cannot explain why the presence of silica has such a profound effect on the magnitude of B. We are carrying out pulsed-laser experiments on these systems to investigate this effect. We anticipate reporting these results in a future publication.

Acknowledgment. The authors thank NSERC Canada and Materials and Manufacturing Ontario (MMO) for their support of this work.

References and Notes

(1) For example, see: (a) Wu, S. *Polymer* **1985**, *26*, 1855. (b) Vollenberg, P. T. H.; Heikens, D. *Polymer* **1989**, *30*, 1656. (c) Stricker, F.; Bruch, M.; Mülhaupt, R. *Polymer* **1997**, *38* (21), 5347.

(2) (a) Cox, M. E.; Dunn, B. *J. Polym. Sci., Part A: Polym. Chem.* **1986**, *24*, 2395. (b) Gouin, S.; Gouterman, M. *J. Appl. Polym. Sci.* **2000**, *77*, 2824.
(3) (a) Xu, W.; McDonough, R. C., III; Langsdorf, B.; Demas, J. N.; Degraff, B. A. *Anal. Chem.* **1994**, *66*, 4133. (b) Demas, J. N.; DeGraff, B. A. *J. Chem. Edu.* **1997**, *74* (6), 690.
(4) Preininger, C.; Klimant, I.; Wolfbeis, O. S. *Anal. Chem.* **1994**, *66*, 1841.
(5) (a) Hartmann, P.; Leiner, M. J. P.; Lippitsch, M. E. *Sensors Actuators B* **1995**, *29*, 251. He, H.; Fraatz, R. J.; Leiner, M. J. P.; Rehn, M. M.; Tusa, J. K. *Sensors Actuators B* **1995**, *29*, 246.
(6) Chan, C.; Chan, M.; Zhang, M.; Lo, W.; Wong, K. *Analyst* **1999**, *124*, 691.
(7) Long, D.; Lequeux, F. *Eur. Phys. J.* **2000**, in press.
(8) (a) Paul, D. R.; Kemp, D. R. *J. Polym. Sci., Polym. Symp.* **1973**, *41*, 79. (b) Van Amerongen, G. J. *Rubber Chem. Technol.* **1964**, *37*, 1067. (c) Kamiya, Y.; Naito, Y.; Hirose, T.; Mizoguchi, K. *J. Polym. Sci. B: Polym. Phys.* **1990**, *28*, 1297.
(9) (a) James, D. R.; Liu, Y. S.; DeMayo, P.; Ware, W. R. *Chem. Phys. Lett.* **1983**, *20*, 460. (b) Chu, D. Y.; Thomas, J. K. *Macromolecules* **1988**, *21*, 2094.
(10) (a) Kavandi, J.; Callis, J.; Gouterman, M.; Khali, G.; Green, E.; Burns, D.; McLachlan, B. *Rev. Sci. Instrum.* **1990**, *61* (11), 3340. (b) Gouterman, M. *J. Chem. Edu.* **1997**, *74* (6), 697.
(11) (a) Kavandi, J.; Callis, J.; Gouterman, M.; Khali, G.; Green, E.; Burns, D.; McLachlan, B. *Rev. Sci. Instrum.* **1990**, *61* (11), 3340. (b) Gouterman, M. *J. Chem. Edu.* **1997**, *74* (6), 697.
(12) Moshasrov, V.; Radchenko, V.; Fonov, S. *Luminescent Pressure Sensors in Aerodynamic Experiments*; Central Aerodynamic Institute (TsAGI): Moscow, 1998.
(13) (a) Lu, X.; Winnik, M. A. Luminescence Quenching by Oxygen in Polymer Films. In *Molecular and Supramolecular Photochemistry*; Ramamurthy, V., Schanze, K. S., Eds.; Marcel-Dekker, New York, 2000; Vol. 6, pp 311−352. (b) Masoumi, Z.; Stoeva, V.; Yekta, A.; Winnik, M. A.; Manners, I. Studies of Oxygen Diffusion in Polysiloxane Resins with Application to Luminescence Barometry. In *Polymers and Organic Solids*; Shi, L., Zhu, D., Eds.; Science Press: Beijing, 1997; pp 157−168.
(14) (a) Puklin, E.; Carlson, B.; Gouin, S.; Costin, C.; Green, E.; Ponomarev, S.; Tanji, H.; Gouterman, M. *J. Appl. Polym. Sci.* **2000**, *77*, 2795. (b) Gouin, S.; Gouterman, M. *J. Appl. Polym. Sci.* **2000**, *77*, 2805.
(15) (a) Liang, M.; Manners, I. *J. Am. Chem. Soc.* **1991**, *113*, 4044. (b) Ni, Y.; Stammer, A.; Liang, M.; Massey, J.; Vancso, G. J.; Manners, I. *Macromolecules* **1992**, *25*, 7119. (c) Ni, Y.; Park, P.; Liang, M.; Massey, J.; Waddling, C.; Manners, I. *Macromolecules* **1996**, *29*, 3401.
(16) (a) Masoumi, Z.; Stoeva, V.; Yekta, A.; Pang, Z.; Manners, I.; Winnik, M. A. *Chem. Phys. Lett.* **1996**, *261*, 551. (b) Pang, Z.; Gu, X.; Yekta, A.; Masoumi, Z.; Coll, J. B.; Winnik, M. A.; Manners, I. *Adv. Mater.* **1996**, *8* (9), 768. (c) Jayarajah, C. N. M.S. Thesis, University of Toronto, 1998. (d) Jayarajah, C. N.; Yekta, A.; Manners, I.; Winnik, M. A. *Macromolecules* **2000**, *33* (15), 5693. (e) Ruffolo, R.; Evans, C.; Liu, X. H.; Ni, Y.; Pang, Z.; Park, P.; McWilliams, A.; Gu, X.; Lu, X.; Yekta, A.; Winnik, M. A.; Manners, I. *Anal. Chem.* **2000**, *72*, 1894.
(17) The refractive index of silica depends on the type of silica, with values ranging from 1.45−1.48: Kretz, R. In *Handbook of Chemistry and Physics*, 75th ed.; Lide, D. R., Frederikse, H. P. R., Eds.; CRC Press: Boca Raton, FL, 1995; pp 4−148.
(18) Miller, R. L. In *Polymer Handbook*, 4th ed.; Brandrup, J., Immergut, E. H., Grulke, E. A., Eds.; Wiley: New York, 1999; p VI−69.
(19) Yekta, A.; Masoumi, Z.; Winnik, M. A. *Can. J. Chem.* **1995**, *73*, 2021.
(20) Nowakowska, P. F.; Najbar, J.; Waligoa, B. *Eur. Polym.* **1976**, *12*, 387.
(21) Guillet, J. E.; Andrews. M. *Macromolecules* **1992**, *25*, 2752.
(22) See: Stanislawska, A.; LePoutre, P. In *Technology for Waterborne Coatings*; Glass, J. E., Ed.; ACS Symp. Ser. 663; American Chemical Society: Washington, D.C., 1997; p 226.
(23) Pauly, S. In *Polymer Handbook*, 4th ed.; Brandrup, J., Immergut, E. H., Grulke, E. A., Eds.; Wiley-Interscience: New York, 1989; p VI−559.
(24) (a) Chambers, W. R.; Kearns, D. R. *J. Phys. Chem*, **1968**, *72*, 4718. (b) Valdes-Aquilera, O.; Neckers, D. *Acc. Chem. Res.* **1989**, *22*, 171. (c) Sathy, P.; Penzkofer, A. *J. Photochem. Photobiol. A: Chem.* **1997**, *109*, 53.
(25) Levin, P. P.; Costa, S. M. B.; Ferreira, L. F. V.; Lopes, J. M.; Ribeiro, F. R. *J. Phys. Chem. B.* **1997**, *101*, 1355. (b) Levin, P. P.; Costa, S. M. B.; Lopes, J. M.; Serralha, F. N.; Ribeiro, F. R. *Spectrochim. Acta A*, **2000**, *56* (9), 1745.
(26) Levin, P. P.; Costa, S. M. B. *Chem. Phys. Lett* **2000**, *320* (1−2) 194.
(27) Springob, C.; Wolff, T. *J. Photochem. Photobiol. A: Chem.* **1996**, *101*, 75.
(28) (a) Sacksteder, L.; Demas, J. N.; DeGraff, B. A. *Anal. Chem.* **1993**, *65*, 3480. (b) Carraway, E. R.; Demas, J. N.; DeGraff, B. A. *Langumir* **1991**, *7*, 2991.
(29) Klimant, I.; Leiner, M. J. P. *Abstracts*, 1st European Conference on Optical Chemical Sensors and Biosensors; Graz, Austria, April 12−15, 1992; p 131.
(30) Lu, X.; Manners, I.; Winnik, M. A., unpublished observations.
(31) Mackie, J. S.; Meares, P. *Proc. R. Soc. London A* **1955**, *232*, 498.
(32) Martinho, J. M. G.; Tencer, M.; Campos, M.; Winnik, M. A. *Macromolecules* **1989,** *22*, 322.

MA001454J